UC Irvine
UC Irvine Previously Published Works

Title

In-depth analysis of pH-dependent mechanisms of electromechanical reshaping of rabbit nasal septal cartilage.

Permalink

Journal

ISSN

Authors

Kuan, Edward C
Hamamoto, Ashley A
Manuel, Cyrus T
et al.

Publication Date

DOI

Copyright Information

Peer reviewed

In-Depth Analysis of pH-dependent Mechanisms of Electromechanical Reshaping of Rabbit Nasal Septal Cartilage

Edward C. Kuan, MD, MBA, **Ashley A. Hamamoto, BS**, **Cyrus T. Manuel, BS**, **Dmitriy E. Protsenko, PhD**, and **Brian J.F. Wong, MD, PhD**

Department of Head and Neck Surgery, University of California–Los Angeles (E.C.W.), Los Angeles; and the Beckman Laser Institute and Medical Clinic, University of California–Irvine (E.C.W., A.A.H., C.T.M., D.E.P., B.J.F.W.), Irvine, California, U.S.A.

Abstract

Objectives/Hypothesis—Electromechanical reshaping (EMR) involves reshaping cartilage by mechanical deformation and delivering electric current to the area around the bend axis, causing local stress relaxation and permanent shape change. The mechanism of EMR is currently unclear, although preliminary studies suggest that voltage and application time are directly related to the concentration and diffusion of acid–base products within the treated tissue with little heat generation. This study aims to characterize local tissue pH changes following EMR and to demonstrate that local tissue pH changes are correlated with tissue damage and shape change.

Study Design—Ex vivo animal study involving EMR of rabbit nasal septal cartilage and biochemical estimation of tissue pH changes.

Methods—The magnitude and diffusion of acid–base chemical products in control (0V, 2 minutes), shape change (4V, 4 minutes; 6V, 1, 2, 4 minutes; 8V, 1, 2 minutes), and tissue damage (8V, 4, 5 minutes; 10V, 4, 5 minutes) parameters following EMR are approximated by analyzing local pH changes after pH indicator application.

Results—There is a direct relationship between total charge transfer and extent of acid–base product diffusion ($P < 0.05$). A "pH transition zone" is seen surrounding the bend apex above 8V, 2 minutes. Colorimetric analysis suggests that small local pH changes (10^{-8} hydrogen ions) are at least partly implicated in clinically efficacious EMR.

Conclusions—These results provide additional insight into the translational applications of EMR, particularly the relationship among pH changes, shape change, and tissue injury, and are integral in optimizing this promising technology for clinical use.

Keywords

Cartilage reshaping; electromechanical; pH; basic science

Introduction

Congenital, iatrogenic, inflammatory, and traumatic defects often damage cartilage in head, neck, and upper airway, resulting in significant functional and aesthetic consequences. Traditional repair involves sculpting, cutting, and transplanting cartilage allografts, which created variable results depending on the preferences and skills of the surgeon. An alternative, minimally invasive modality that has received some attention is laser cartilage reshaping (LCR). In LCR[1–5] as well as other thermal-based reshaping mechanisms (i.e., radiofrequency cartilage reshaping[6]), thermal-mediated stress relaxation produces permanent, quantifiable, and consistent shape change, but at the expense of local tissue injury.

In electromechanical reshaping (EMR), electrical current is applied to platinum needle electrodes inserted into regions of user-defined tissue deformation, leading to sustained shape change. EMR is the latest emerging cartilage reshaping modality.[7–9] EMR provides multiple advantages over traditional techniques and also LCR, including its minimally invasive nature, dependence on voltage and application time[8] as well as electrode geometry,[9] and dependence on a nonthermal electrochemical mechanism.[7] Component costs are inexpensive, on par with sutures. It is speculated, at least as part of the mechanism of EMR, that oxidation-reduction (redox) reactions occur at the tissue–electrode interface, producing H^+ and OH^- ions at the anode and cathode ends, respectively, that interact with ionic bonds within the cartilage matrix and result in permanent changes in tissue biomechanics.[10,11]

Herein, we have studied the relationship between needle electrode-based EMR shape change in rabbit nasal septal cartilage and spatially localized changes in pH. Building on previous work in our laboratory, we conduct an analysis of the pH-based mechanisms of EMR. The aims of this study include: 1) characterize local tissue pH changes following EMR, 2) demonstrate that local tissue pH changes are correlated with tissue damage, and 3) demonstrate that local tissue pH changes are correlated with shape change.

Materials and Methods

Specimen Preparation

This protocol has been approved by the University of California–Irvine Institutional Review Board and Institutional Animal Care and Use Committee. Fresh rabbit crania were obtained from a local abattoir. Nasal septal cartilage was harvested and each specimen cleaned and trimmed to standard dimensions used in previous EMR experiments ($20 \times 8 \times 1$ mm).[7,12]

Electromechanical Reshaping

Standardized tissue specimens are secured in a precision-machined mechanical jig with a 90° bend angle. Three platinum needle electrodes in an array parallel to the axis of the bend are inserted on opposite ends of the bend apex through precision-machined slots such that the distance between arrays of electrodes is 6 mm. User-defined voltage and application times are set to control, shape change, or tissue damage parameters (n = 5–6 per parameter set, described below) and direct current is channeled through the cartilage sample. The aforementioned parameters were determined based on findings from previous EMR experiments.[7,9,12]

- Controls (0 V, 2 minutes): Electrodes inserted, but no current applied. Controls assess the effects of mechanical stress on tissue reshaping. Because there is no electrical current delivered to the specimen, no local pH changes—and thus no color changes—would be expected occur (i.e., sample would remain pink from natural color of pH indicator).[13]

- Shape change (4 V, 4 minutes; 6 V, 1, 2, 4 minutes; 8 V, 1 minute): Includes voltages and application times within which cartilage tissue is statistically significantly reshaped (but without tissue injury) for potential clinical use.[9]

- Tissue damage (8 V, 4, 5 minutes; 10 V, 4, 5 minutes): Includes those voltages and application times at or marginally higher than those parameters previously found to produce maximal shape change with noted tissue damage.[9]

After the designated time of voltage application elapsed, each specimen was rehydrated with its shape retained within the jig in phosphate buffered saline, pH 7.4, for approximately 1 minute to simulate physiologic re-equilibration of normal tissue ionic state. We have previously found that rehydration has a minimal impact on the ability to visualize pH indicator-induced color changes in cartilage specimens; therefore, we have elected to rehydrate each specimen only briefly.[13]

Application of pH Indicator

Each rehydrated specimen was removed from the jig, and phenol red pH indicator solution (Invitrogen Corporation, Carlsbad, CA) was applied directly to the bent specimen, observing for color changes to estimate pH changes. Phenol red appears yellow below a pH range of 6.8 to 8.4 and appears pink above it. Each specimen was incubated in phenol red for approximately 1 minute; pilot studies have shown that such a time frame is adequate to yield color changes evident at an incubation time as long as 15 minutes.[13]

Specimen Photography

Cartilage specimens are photographed (Rebel XS EOS, Canon USA, Melville, NY) atop an x-ray film viewbox for proper backlighting (specimens are translucent) after stable color change is observed. A ruled scale was included in each photograph to allow for approximation of distance of pH indicator diffusion. A polarizing filter was used over the camera lens to minimize specular reflection.

Data Analysis

Color changes observed in controls, if any, were compared with color changes observed in EMR-treated specimens, and specimens treated with different EMR voltage and time parameters were compared to each other. Intensity of color changes in EMR-treated specimens were correlated to pH changes by a pH calibration scale (Fig. 1). The pH calibration scale was derived by incubating control rabbit nasal septal cartilage specimens for 24 hours in custom-made solutions of various pHs (<5, 5.8, 6.4, 7.0, 7.6, 8.0, >8). A phenol red pH indicator was applied to each specimen, and color changes corresponding to tissue pH changes were noted. Local color changes observed after application of pH indicator to EMR-treated samples were compared to this scale, which can roughly quantify local pH changes following EMR. This color scale was also photographed over the same x-ray film viewbox to ensure consistency of color assessment between samples and standards.

Areas of pH change for the shape change and tissue damage parameters were analyzed using the measure tool in NIH ImageJ (Bethesda, MD) based on a previous protocol,[13] allowing for quantification of the lateral distance (in mm) of color change from the bend axis. Measured areas of pH change can also be compared between samples treated using different EMR voltage and time parameters, as the distribution of local pH change is expected to differ with different parameters. A photograph of a sample specimen and the analysis involved is shown in Figure 2.

Descriptive statistics (mean and standard deviation) were used in summarizing measured areas of pH change (pink L, pink R, yellow L, yellow R, transition zone [TZ]). Single-factor analysis of variances (Microsoft Excel, Redmond, WA) was used to compare differences in areas of pH change among samples treated with the same voltage and time parameter set to ensure experimental precision (e.g., all 5 samples treated with 6 V, 2 minutes). Once precision was confirmed, we used two-tailed Student t tests to compare differences in areas of pH change between tissue damage and shape change parameter sets (e.g., 6 V, 2 minutes vs. 6 V, 4 minutes). Linear regression using total charge transfer (as a function of current transferred and application time, calculated from a previously established protocol[7,12]) as the independent variable and lateral extent of diffusion as the dependent variable was performed. A significance level of 0.05 was used for all statistical testing.

Because there are no commercial pH meters/probes that can exactly quantify cartilage tissue pH; pH can only be estimated from the intensity of color change correlating to the pH calibration scale. The colors of red, green, and blue may be described using the hue-saturation-brightness (HSB) coordinate system, in which the "uniqueness" of each color is principally quantified using the hue parameter. ImageJ was used to measure hue for each HGB-stacked colored specimen in the pH calibration scale. A rough standardization curve indicating a polynomial relationship between tissue pH and hue was generated using Excel's trendline function (Fig. 3).

Hue indices were then measured for control and EMR-treated cartilage samples (n = 3 samples per parameter set) in local regions of color change (i.e., both pink and yellow areas, corresponding to cathode and anode, respectively) and summarized using descriptive statistics. Approximate tissue pH values were extrapolated from the above standardization

curve using the goal seek function in Excel based on the measured hue indices for each sample.

Results

Diffusion of Redox Products

The extents of diffusion (as a correlate of the extent of redox products diffusion within the cartilage tissue matrix) are indicated in Table I. A TZ was not noted for specimens treated under 8 V, 2 minutes, but consistently observed above this threshold value. Analysis of variance revealed no significant differences in measurements of color change between samples treated by similar voltage and time parameters, indicating that measurements were taken with reasonable precision.

Diffusion as Function of Total Charge Transfer

There is a statistically significant relationship between total charge transfer (in Table I) and diffusion of redox products as manifested by areas of color change ($P = 0.0001$, 0.12, 0.007, and 0.0008 for pink L, pink R, TZ, yellow L, and yellow R respectively). The R^2 values for pink L, pink R, TZ, yellow L, and yellow R as a function of total charge transfer were 0.85, 0.27, 0.62, and 0.78, respectively. For parameters that produced a TZ at the bend apex, there appears to be a statistically significant relationship between total charge transfer and size of the TZ ($P = 0.007$), with an R^2 value of 0.93.

Quantifiable pH Change

Hue indices were directly measured in the center portions of each area of color change following EMR and application of the pH indicator. Approximate pH values were derived from the standardization curve. For tissue damage parameters, hue was also measured for the TZ, and approximate pH values were extrapolated. The results are reported in Table II.

Discussion

EMR is a promising new modality for minimally invasive reshaping of cartilage tissues in the head and neck. In EMR, cartilage tissue is mechanically deformed and direct current is delivered to the specimen for a user-defined application time. Changes in biomechanical properties occur at the apex of the bend, which corresponds to the region between opposite polarity electrodes and the area of maximal mechanical stress. Early mechanistic studies based on EMR using flat-plate electrodes revealed that EMR generates negligible heat (less than 1°C) and results in the hydrolysis of water and evolution of oxygen, hydrogen, and chlorine gases (local bubble formation).[7] These observations suggest that EMR operates through a nonthermal mechanism that likely involves redox reaction formation (i.e., the foam and bubbles are redox byproducts) with concomitant local pH changes.[7] As a result, an understanding of the role of pH changes in EMR is critical in helping predict the extent of tissue damage following EMR. This relationship is, at the very best, currently unclear. Since its inception, EMR and its potential clinical applications have been studied extensively. Prior studies have explored the relationship between dosimetry and shape change[7–9,12,14]; changes in tissue biomechanics[15]; posttreatment and long-term tissue viability[16–18]; ex vivo

tissue experiments mimicking human operations[19,20]; and more recently, in vivo investigations.[18,21] Despite the growing body of literature surrounding EMR, no formal mechanistic studies have been attempted until now. The current study aims to fill a void in the EMR literature and is the first mechanistic study to rigorously explore the relationship among local pH change, shape change, and expected tissue injury.

Contemporary understanding of cartilage tissue behavior under mechanical stress is largely based on Lai's triphasic theory, which states that the biomechanical properties of cartilage tissue are dependent on fixed charge density (e.g., proteoglycans), the stiffness of the collagen matrix, and interstitial ionic content.[22] EMR, which essentially transforms deformed cartilage tissue into an electrochemical cell, is postulated to directly affect interstitial ionic content, where the ions are free-flowing within a fluid medium.[23] Thus, acid–base products (hydroxyl ion at the cathode and hydrogen ion at the anode) formed at the tissue–electrode interface diffuse through the interstitial fluid as its ionic concentration changes over time with the overlying electric field, resulting in areas lateral to and between arrays of electrodes in which pH indicator may be applied to detect the presence of acid–base products.

In this study, we noted a statistically significant, direct relationship between voltage and time with the extent of lateral color diffusion following EMR, indicating again that acid–base products generated at the tissue–electrode interface travel distally in the area of the electric field. It is hypothesized that, with increasing voltage, charge is increasingly delivered to the tissue–electrode interface, which accelerates the reaction rate by which the acid–base products are formed. As a result, generation of more products within a larger electric field concomitantly increases the rate of diffusion, which may account for the more expansive area of color change with higher voltage parameters.[14] Similarly, with increasing application time, redox reactions are able to proceed to completion, which is speculated to also increase the local concentration of acid–base products, explaining the increased areas of color change.[14] Furthermore, there is a direct relationship between voltage and time parameters and the intensity of color change, which is accounted for by a similar mechanism (i.e., increased concentration of redox products results in increased interactions with the pH indicator dye, producing color change). Taken together, these phenomena suggest that an increase in voltage and/or application time results in both 1) increased diffusion and 2) increased local concentrations of redox products.

At 8 V, 2 minutes and above, there exists a TZ in which the acidic and basic products mix around the apex of the bend. This was noted in pilot studies[13] and, upon further investigation of a more expansive parameter set, appears to predominate in specimens treated by parameters that are known to produce tissue injury. One possible explanation is that high concentrations of redox products overlap in the TZ, rendering it an area highly saturated by strong acids (H^+) and bases (OH^-). The end result is a caustic microenvironment around the area of the bend, which causes local tissue denaturation and manifests as gross tissue injury. Thus, in order to optimize EMR for safe clinical use, parameters that produce a TZ in the apex should be avoided or utilized with caution.

A very basic colorimetric analysis using a measured relationship between hue and tissue pH was performed in this study. Accordingly, control samples have an estimated tissue pH of 7.4, which is physiological. It appears that the magnitude of pH change following EMR is rather small (on the order of $\pm 10^{-2}$ pH units, or a gain/loss of 10^{-8} M H$^+$), suggesting that at least partly the minor alterations in tissue ionic content in the setting of mechanical deformation may be sufficient for shape change—and possibly even tissue injury based on previously known damage thresholds.[7] This may be attributable to the low magnitude of charge transfer described in previous EMR studies (on the order of 0.01 mC).[7,9] Although the extrapolated pH values provide some insight into the magnitude of pH changes necessary to produce shape change without tissue injury, the current approach is limited by the use of a single pH indicator because more extreme pH values (i.e., those outside of the indicator's buffer range) may not be accurately quantified (e.g., for phenol red, the hue indices at pH 3 and 5 would be indistinguishable). One possible consideration is to repeat the analysis with multiple pH indicators (e.g., thymol blue, methyl red) to increase colorimetric resolution, although the same limitation would apply for extreme pH values (although likely clinically insignificant).

There are several limitations to the current study. First, we did not evaluate post-EMR tissue changes using histological or other means of viability analysis. We have previously studied the effect of EMR on cartilage tissue based on both classic histology[21] and fluorescence laser scanning confocal microscopy.[16–18] These studies indicate that EMR preserves epidermal and adnexal structures while stimulating local neochondrogenesis, with a chondrocyte viability rate roughly comparable to that in traditional reshaping techniques (e.g., morselization). In fact, the region of injury surrounding percutaneously placed needle electrodes is less than 2.5 mm in diameter for the electrical dosimetry parameters evaluated.[18] Furthermore, in these earlier publications, no additional signs of unexpected nonthermal injury were found in histological analysis. As the current study involves experiments performed in a similar manner (with near identical electrical dosimetry) to those used in both previous in vivo and ex vivo studies (with the simple addition of adding pH indicator), we elected not to repeat these studies.

Second, the current study does not include additional information on biomechanical properties of EMR-treated tissues, which we have studied in the past, albeit under different geometric conditions to facilitate detailed mechanical analysis.[15] At best, the EMR of rabbit nasal septal cartilage produces a modest level of reduction in elastic modulus within clinically applicable parameters, while largely preserving the overall structural integrity of the tissue. This is in contrast to traditional, more destructive means of reshaping cartilage that include cutting, carving, and suturing, which inevitably disrupt tissue structure and also produce unwanted changes in biomechanical properties. In vivo investigations involving the biomechanical testing of EMR-treated cartilage are in progress.

Third, the current study does not evaluate long-term cartilage behavior in an in vivo setting. In vivo investigation of EMR has been performed in using both rabbit auricular cartilage to mimic otoplasty[18,21] and rabbit costal cartilage simulating microtia repair.[16,20] These studies demonstrated sustained shape change 4 weeks after treatment, with chondrocyte loss only in the vicinity immediately adjacent to the electrodes where significant pH changes are thought

to occur. The previous studies suggest that shape change is clinically significant and demonstrates the potential long-term feasibility of EMR. In addition, given the larger sample sizes necessary to detect differences between treatment parameters, ex vivo evaluation was deemed more time-effective and cost-effective for this mechanistic study. pH changes modify the biomechanical properties of cartilage; specifically, there is an inverse relationship between cartilage tissue pH and tissue elastic modulus.[11,24] Beyond certain changes in elastic modulus, cartilage tissue becomes irreversibly damaged (an undesired clinical outcome), and the threshold values above which this takes place are known.[15] Thus, understanding pH changes following EMR and its relationship with undesirable tissue injury, especially when coupled with data on cartilage viability following EMR, is highly impactful and provides significant insight on how to optimize EMR technology for safe and efficacious clinical application.

Conclusion

The current study is the first mechanistic exploration on the topic to provide some valuable insight into the basic science mechanisms of EMR, which in turn may better elucidate the relationship among local pH change, clinically significant reshaping, and thermal injury. Thus, it may serve as the basis for future investigations into optimizing this promising technology for safe, efficacious clinical use.

Acknowledgments

Bibliography

1. Gorgu M, Ayhan M, Aslan G, Erdogan B, Tuncel A. Cartilage shaping using the Er:YAG laser: preliminary report. Ann Plast Surg. 2000; 45:150–154. [PubMed: 10949342]

2. Ayhan M, Deren O, Gorgu M, Erdogan B, Dursun A. Cartilage shaping with the Er:YAG laser: an in vivo experimental study. Ann Plast Surg. 2002; 49:527–531. [PubMed: 12439022]

3. Helidonis E, Sobol E, Kavvalos G, et al. Laser shaping of composite cartilage grafts. Am J Otolaryngol. 1993; 14:410–412. [PubMed: 8285311]

4. Jones N, Sviridov A, Sobol E, Omelchenko A, Lowe J. A prospective randomised study of laser reshaping of cartilage in vivo. Lasers Med Sci. 2001; 16:284–90. [PubMed: 11702634]

5. Ovchinnikov Y, Sobol E, Svistushkin V, Shekhter A, Bagratashvili V, Sviridov A. Laser septochondrocorrection. Arch Facial Plast Surg. 2002; 4:180–185. [PubMed: 12167077]

6. Keefe MW, Rasouli A, Telenkov SA, et al. Radiofrequency cartilage reshaping: efficacy, biophysical measurements, and tissue viability. Arch Facial Plast Surg. 2003; 5:46–52. [PubMed: 12533139]

7. Protsenko DE, Ho K, Wong BJ. Stress relaxation in porcine septal cartilage during electromechanical reshaping: mechanical and electrical responses. Ann Biomed Eng. 2006; 34:455–464. [PubMed: 16450186]

8. Ho KH, Diaz Valdes SH, Protsenko DE, Aguilar G, Wong BJ. Electromechanical reshaping of septal cartilage. Laryngoscope. 2003; 113:1916–1921. [PubMed: 14603047]

9. Wu EC, Khan A, Protsenko DE, et al. Electromechanical reshaping of rabbit septal cartilage: a six needle electrode geometric configuration. Proc Soc Photo Opt Instrum Eng. 2009; 7161

10. Frank EH, Grodzinsky AJ. Cartilage electromechanics—I. Electrokinetic transduction and the effects of electrolyte pH and ionic strength. J Biomech. 1987; 20:615–627. [PubMed: 3611137]

11. Eisenberg SR, Grodzinsky AJ. The kinetics of chemically induced nonequilibrium swelling of articular cartilage and corneal stroma. J Biomech Eng. 1987; 109:79–89. [PubMed: 3560885]

12. Manuel CT, Foulad A, Protsenko DE, Sepehr A, Wong BJ. Needle electrode-based electromechanical reshaping of cartilage. Ann Biomed Eng. 2010; 38:3389–3397. [PubMed: 20614240]

13. Wu EC, Manuel CT, Protsenko DE, Karimi K, Hamamoto A, Wong BJ. pH-dependent mechanisms of electromechanical cartilage reshaping. Proc Soc Photo Opt Instrum Eng. 2011; 7883

14. Wu EC, Protsenko DE, Khan AZ, Dubin S, Karimi K, Wong BJ. Needle electrode-based electromechanical reshaping of rabbit septal cartilage: a systematic evaluation. IEEE Trans Biomed Eng. 2011; 58:8. Epub 2011. 10.1109/TBME.2011.2157155

15. Lim A, Protsenko DE, Wong BJ. Changes in the tangent modulus of rabbit septal and auricular cartilage following electromechanical reshaping. J Biomech Eng. 2011; 133:094502. [PubMed: 22010748]

16. Badran K, Manuel C, Waki C, Protsenko D, Wong BJ. Ex vivo electromechanical reshaping of costal cartilage in the New Zealand white rabbit model. Laryngoscope. 2013; 123:1143–1148. [PubMed: 23553270]

17. Protsenko DE, Ho K, Wong BJ. Survival of chondrocytes in rabbit septal cartilage after electromechanical reshaping. Ann Biomed Eng. 2011; 39:66–74. [PubMed: 20842431]

18. Yau AY, Manuel C, Hussain S, Protsenko D, Wong BJ. In vivo needle-based electromechanical reshaing of pinnae: New Zealand white rabbit model. JAMA Facial Plast Surg. 2014 In press.

19. Manuel CT, Foulad A, Protsenko DE, Hamamoto A, Wong BJ. Electromechanical reshaping of costal cartilage grafts: a new surgical treatment modality. Laryngoscope. 2011; 121:1839–1842. [PubMed: 22024834]

20. Badran KW, Waki C, Hamamoto A, Manz R, Wong BJ. The rabbit costal cartilage reconstructive surgical model. Facial Plast Surg. 2014; 30:76–80. [PubMed: 24488642]

21. Oliaei S, Manuel C, Karam B, et al. In vivo electromechanical reshaping of ear cartilage in a rabbit model: a minimally invasive approach for otoplasty. JAMA Facial Plast Surg. 2013; 15:34–38. [PubMed: 23117484]

22. Lai WM, Hou JS, Mow VC. A triphasic theory for the swelling and deformation behaviors of articular cartilage. J Biomech Eng. 1991; 113:245–258. [PubMed: 1921350]

23. Protsenko DE, Lim A, Wu EC, Manuel CT, Wong BJ. The influence of electric charge transferred during electro-mechanical reshaping on mechanical behavior of cartilage. Proc Soc Photo Opt Instrum Eng. 2011; 7901

24. Myers TG, Aldis GK, Naili S. Ion induced deformation of soft tissue. Bull Math Biol. 1995; 57:77–98. [PubMed: 7833853]
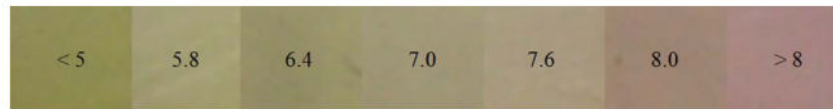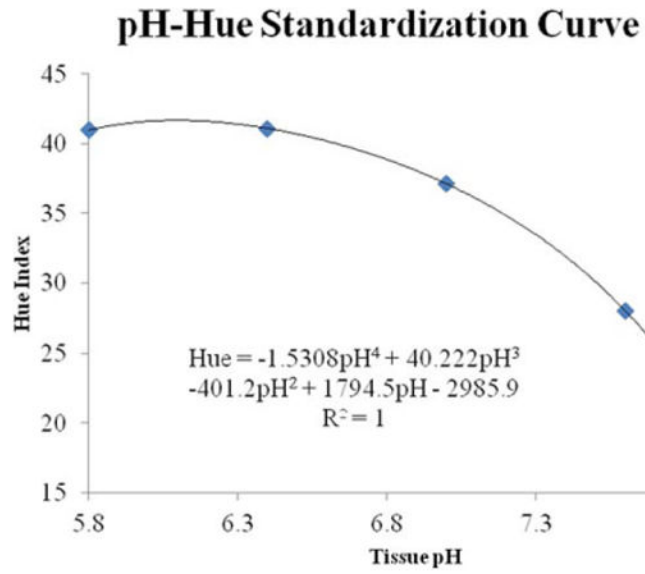
Fig. 1.
pH calibration scale. Native cartilage tissue was incubated in custom pH solutions, indicated by values above, with corresponding color change following treatment with phenol red pH indicator. [Color figure can be viewed in the online issue, which is available at wileyonlinelibrary.com.]
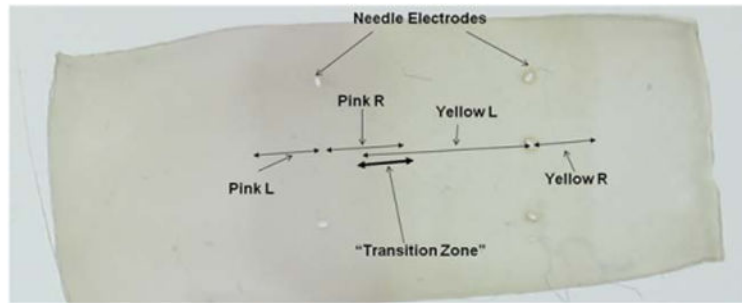
Fig. 2.
Analysis of areas of color change in an actual electromechanical reshaping-treated (8 V, 4 minutes), phenol red-treated tissue specimen. A ruler (not shown) was included in each photograph for measuring purposes. Note the "transition zone" near the bend apex reflecting the blending of pink and yellow areas.

pink L = left-lateral limit of pink color change; pink R = right-lateral limit of pink color change; yellow L = left-lateral limit of yellow color change; yellow R = right-lateral limit of yellow color change. [Color figure can be viewed in the online issue, which is available at wileyonlinelibrary.com.]

pH-Hue Standardization Curve

$$Hue = -1.5308pH^4 + 40.222pH^3 - 401.2pH^2 + 1794.5pH - 2985.9$$
$$R^2 = 1$$

Fig. 3.

pH-hue standardization curve based on known pH value and hue-measured local tissue color change from pH calibration scale (Fig. 1). This curve allows for a rough extrapolation of tissue pH given hue, or vice versa. [Color figure can be viewed in the online issue, which is available at wileyonlinelibrary.com.]

Table I

The Measured Areas of Color Change as a Function of Voltage and Time.

					Shape Change				
Voltage (V)	Time (min)	n	Charge (kC)	Pink L (mm)	Pink R (mm)	TZ (mm)	Yellow L (mm)	Yellow R (mm)	ANOVA P
4	4	5	0.18	1.11±0.10	1.22±0.19	0	0.93±0.14	0.85±0.12	0.29
6	1	6	0.10	1.15±0.27	1.25±0.15	0	1.22±0.14	0.98±0.16	0.40
6	2	6	0.20	1.52±0.26	1.92±0.20	0	1.71±0.13	1.27±0.19	0.35
6	4	5	1.16	2.35±0.30	2.68±0.44	0	2.93±0.30	1.66±0.27	0.99
8	1	5	0.20	1.67±0.15	2.05±0.10	0	1.74±0.33	1.41±0.30	0.40
8	2	5	0.79	1.65±0.31	2.63±0.39	0.72±0.15	2.77±0.38	1.60±0.33	0.98

					Tissue Damage				
Voltage (V)	Time (min)	n	Charge (kC)	Pink L (mm)	Pink R (mm)	TZ (mm)	Yellow L (mm)	Yellow R (mm)	ANOVA P
8	4	5	2.38	2.38±0.74	2.71±0.71	1.10±0.21	3.88±0.46	2.39±0.62	0.98
8	5	5	4.81	2.75±0.35	2.35±0.42	1.34±0.48	3.35±0.85	2.13±0.25	0.56
10	4	5	5.21	4.36±0.68	2.23±0.25	1.66±0.25	3.29±0.78	2.35±0.49	0.99
10	5	5	5.51	3.58±0.75	2.76±0.58	1.54±0.23	3.74±0.75	2.58±0.71	0.60

Total charge transfer for each parameter set, calculated from previous studies, is provided. ANOVA correlating corresponding color change within each parameter set is indicated in the rightmost column. A significance level of 0.05 was used.

ANOVA = analysis of variance; TZ = transition zone.

Table II

Approximate Local pH Values Extrapolated From Standardization Curve Using Hue Measurements per Voltage and Time Parameter Set.

Control

Voltage (V)	Application Time (min)	Hue Index	Approximate Tissue pH (no EMR performed)
0	2	33.0±3.7	7.4

Shape Change

Voltage (V)	Application Time (min)	Cathode Hue Index	Anode Hue Index	Approximate Cathode pH	Approximate Anode pH
4	4	14.6±2.2	31.7±3.8	8.1	7.4
6	1	14.0±1.7	36.3±0.8	8.1	7.2
6	2	14.0±2.1	35.2±1.0	8.1	7.2

Tissue Damage

Voltage (V)	Application Time (min)	Cathode Hue Index	TZ Hue Index	Anode Hue Index	Approximate Cathode pH	Approximate TZ pH	Approximate Anode pH
8	4	12.1±1.9	23.1±3.2	40.4±1.5	8.1	7.8	6.6
10	5	13.0±0.4	21.8±3.2	38.4±3.7	8.1	7.9	6.9

Note that the pH changes are relatively small H changes.

EMR = electromechanical reshaping; H = hue; TZ = transition zone.